Appl. Phys. B 79, 491–495 (2004)
DOI: 10.1007/s00340-004-1580-9

Applied Physics B
Lasers and Optics

I.S. BURNS
J. HULT
C.F. KAMINSKI✉

Spectroscopic use of a novel blue diode laser in a wavelength region around 450 nm

Department of Chemical Engineering, University of Cambridge, Pembroke Street, Cambridge CB2 3RA, UK

Received: 29 January 2004/Revised version: 7 June 2004
Published online: 20 July 2004 • **© Springer-Verlag 2004**

ABSTRACT This paper reports on the first spectroscopic application of a novel type of GaN blue diode laser emitting around 450 nm, which has recently become available. The diode was characterised and then implemented in an extended cavity, to achieve mode-hop free tuning over a frequency range exceeding 105 GHz. The spectroscopic utility of the device was demonstrated by probing the $5\,^2P_{3/2}$ to $6\,^2S_{1/2}$ transition of atomic indium seeded to an atmospheric pressure flame. Single scans over the pressure broadened hyperfine structure were recorded with high signal-to-noise ratios and profiles of the indium LIF distribution through the flame were acquired, at a high spatial resolution. Potential applications of diodes emitting in this spectral region range from industrial sensing to atomic cooling experiments.

PACS 42.55.Px; 32.50.+d; 42.62.Fi

1 Introduction

Since their invention in the late 1990's [1], GaN diode lasers emitting in the range 390–420 nm have been used in various spectroscopic studies [2–8]. Prior to this, tunable diode laser spectroscopy had been performed principally with red diodes probing electronic transitions in atoms such as Li, Cs or Rb [9, 10], with near infrared diodes probing ro-vibrational overtone transitions of gaseous molecules [11, 12], or with mid-IR diodes probing fundamental vibrational transitions [13, 14]. Devices emitting in the blue and violet part of the spectrum have the advantage that they allow strong electronic transitions to be probed, which, for many atoms of practical interest, were previously inaccessible to diode lasers. This capability has led to the demonstration of laser induced fluorescence (LIF) using diode lasers in the 390–420 nm spectral range in high temperature vapour cells [2], atomic beams [3, 4], and in flames [5]. Atomic species generate strong LIF signals even when excited by low power light sources because their oscillator strengths are typically several orders of magnitude greater than those of molecules. Other applications of violet diode lasers have included absorption spectroscopy of aluminium atoms in a hollow cathode discharge [6] and detection of NO_2 gas at trace concentrations [7]. Violet diode lasers have recently also been employed in atom and ion cooling experiments [8, 15].

In contrast, blue diode lasers operating above 420 nm have not, to the authors' knowledge, been applied in previous spectroscopic studies. This is a spectral region where many interesting species have strong transitions. For applications requiring wavelengths in the region around 450 nm, for example, Nd:YAG laser pumped frequency doubled Ti:Saphire lasers [15], dye lasers [16] or optical parametric oscillators (OPOs) [17] have previously been employed. Continuous wave dye lasers pumped by Ar^+ lasers [18], have also been used in the past. Diode lasers would be an attractive alternative to these systems. The purpose of the present research was to investigate the spectroscopic potential of novel diodes operating in the 430–450 nm wavelength region, which have recently become available [19, 20]. In addition to atomic indium, which has a strong transition in this region (451 nm), NO_2 is another of a target species that could be excited with these sources. Compared to the previously employed solid state or dye lasers, diode lasers are inexpensive, rugged, compact and easily tunable.

In some regions of the red and near infrared spectrum, the manufacture of inherently single mode devices such as distributed feedback (DFB) lasers and vertical cavity surface emitting lasers (VCSEL) has been possible and their use in spectroscopy has become widespread [21, 22]. In the blue and violet spectral region, however, only multi-mode Fabry–Pérot (FP) diodes are commercially available. It is thus necessary to use an extended cavity scheme, employing wavelength selective feedback [9, 23], to obtain narrow linewidth, tunable single-mode emission.

In this paper, we discuss work performed with a diode laser emitting around 450 nm, which constitutes a new wavelength region for diode laser spectroscopy. We report on the longitudinal mode structure of the raw FP device and describe the construction of a wide tuning range extended cavity diode laser (ECDL). The spectral width over which the ECDL can be tuned without mode-hops, is crucial in determining its usefulness for spectroscopic studies. For the extended cavity scheme reported here, this tuning range has been found to exceed 105 GHz. As an example of the practical application of the 450 nm laser, indium fluorescence spectroscopy was performed in an atmospheric pressure flame.

✉ Fax: +44-1223/334-796, E-mail: clemens_kaminski@cheng.cam.ac.uk

2 Experimental set-up

The FP GaN diode laser used was purchased from Nichia Corporation, emitting at around 450 nm and generating an output power of 5 mW when operated at 40 °C. Diode laser injection current and temperature were controlled using commercial drivers (Tektronix, LDC8002 and TED8020). The mode structure of the FP device was resolved and characterised using a 1.26 m spectrograph (Spex) equipped with a back-illuminated, unintensified CCD camera (Wright Instruments, 384 × 576 pixels).

In order to obtain tunable single-mode output, a custom designed extended cavity was constructed around the diode (see Fig. 1). This consisted of an 1800 lines/mm holographic grating (Edmund Scientific) mounted in the Littrow configuration, which served as the frequency selective element and as the output coupler of the extended cavity. The grating was mounted on a three-axis piezo-electric mount (Thorlabs, KC1-PZ) in order that grating angle and cavity length could be tuned independently. Wavelength scanning was achieved by tuning the piezos with two triangular waveforms, which were in phase and whose amplitudes could be accurately adjusted. One of these waveforms was used to modulate the piezo marked 'x' in Fig. 1, and the other was applied to both piezos 'y' and 'z', thus permitting simultaneous rotation and translation of the grating. By contrast, most ECDLs reported [3, 4, 6, 8–10, 24] have been based on mounting a grating on a lever arm and rotating it around a pivot point, the position of which has to be located very precisely to achieve long tuning ranges. The present design avoids the problems of thermal and mechanical instabilities that could result from the lever arm implementation. No anti-reflection coating was applied to the front facet of the diode. Instead the effective length of the internal FP cavity formed by the diode crystal facets was tuned synchronously by ramping the bias current with a third triangular waveform. The output power of the ECDL was around 1 mW. A confocal etalon (FSR = 7.5 GHz; $F = 30$) was used to determine the maximum single-mode wavelength tuning range that could be achieved without mode-hops.

Laser induced fluorescence spectra of indium atoms were recorded in a flame. The experiments were performed in a 10 mm diameter atmospheric pressure laminar CH_4/air Bunsen flame. The air stream was passed through a nebuliser containing an aqueous solution of $InCl_3$, resulting in a concentration of less than 1 ppm of atomic indium in the flame. The output beam from the ECDL was focused to a diameter of 110 μm in the flame. The fluorescence spectrum for the $5\,^2P_{3/2} \rightarrow 6\,^2S_{1/2}$ transition of indium at 451.1 nm was resolved by tuning the laser wavelength over a 40 GHz wide region, at a scan repetition rate of 20 Hz. The resonant fluorescence signal originating from the laser focus was imaged at $f/2.4$ through a pin-hole of 150 μm diameter onto a photomultiplier tube (Hamamatsu, R3788). An interference filter centred around the indium fluorescence transition was used to suppress flame emission. Before entering the flame, part of the laser beam was split off by a glass plate and passed through a solid FP etalon (FSR = 3.1 GHz) to monitor the relative wavelength position, and to ensure that the scan was mode-hop free, A separate photodiode was used continuously to monitor the laser power. The LIF signal, the etalon transmission, the laser intensity, and the modulation waveform were recorded on a PC with a data acquisition card (National Instruments PCI-6014).

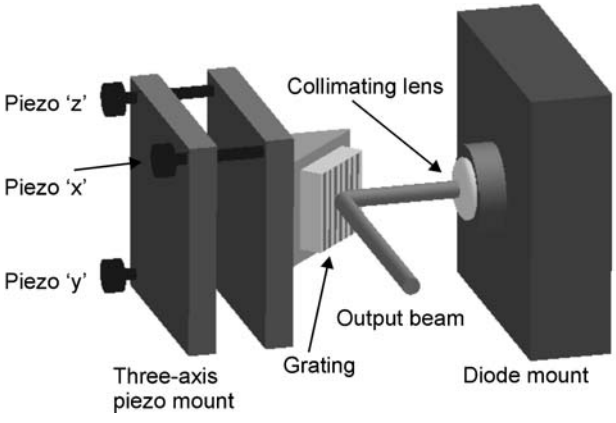

FIGURE 1 The extended-cavity diode laser configuration

3 Results

Figure 2 shows the spectral output from the FP diode laser operating without extended cavity feedback at different diode injection currents ranging from below threshold (45 mA) up to operating current (58 mA). The width of the individual laser modes in the plot is determined by the spectrometer resolution and does not represent the actual linewidth of the laser. The spectrum in plot (a) corresponds to an injection current of 45 mA, which is just below the lasing threshold for a diode operating temperature of 40 °C. Emission from a large number of modes is observed, with a mode spacing of around 0.058 nm. This is in good agreement with the expected FP mode spacing of 0.059 nm for a diode chip length of 0.70 mm [25] at an estimated refractive index of 2.48 [26]. At the threshold current of 46 mA, plot (b), two dominant modes are observed, with a number of weaker side modes present. As the injection current is further increased, plots (c)-(f), the positions of the strongest modes shift to higher wavelengths. Single mode lasing is observed only over limited regions for specific combinations of current and temperature as shown, for example, in plot (c). The observed multimode behaviour is one of the reasons why it is desirable to use the FP laser in an extended cavity configuration for high resolution spectroscopy applications. Another advantage is that the range of coarse wavelength tuning, for a specific diode, can be extended by a few nm beyond what is possible by tuning temperature and current only. The mode spacing observed above threshold current in the present laser matches the regular FP spacing observed below threshold. This is in contrast to previous observations for some violet diode lasers operating in the 400–420 nm region, where mode spacings several times greater than those estimated from the FP cavity length were observed [25, 27].

Figure 3 shows the confocal etalon (FSR = 7.5 GHz; $F = 30$) transmission during a wavelength scan of the ECDL device, in which the diode current was tuned around a central value of 51.9 mA. The 15 etalon fringes observed correspond to mode-hop free tuning over a range exceeding 105 GHz.

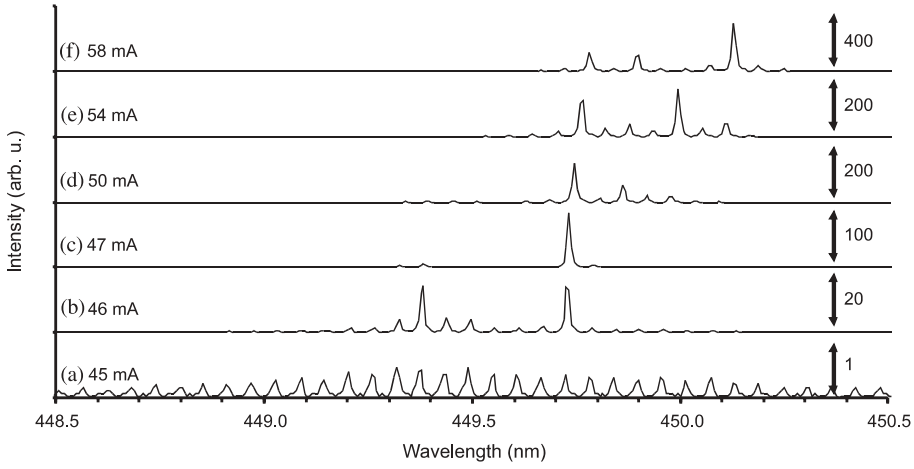

FIGURE 2 Spectral output from the FP diode laser, operating near 451 nm, as a function of diode injection current. (a) corresponds to a current just below the threshold for lasing, (b) is at threshold, and in (c–f) injection currents range from just above threshold up to operating current. The relative intensity scale of each spectrum is indicated to the *right*

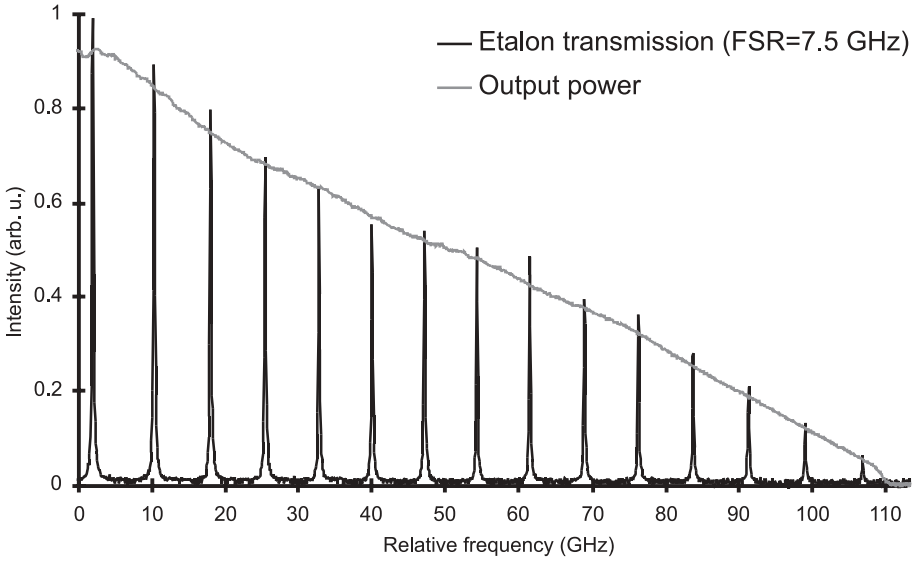

FIGURE 3 Recorded intensity transmitted through a confocal etalon (FSR = 7.5 GHz; $F = 30$) during a single-mode wavelength scan of the ECDL operating near 451 nm. The 15 interference fringes observed correspond to a mode-hop free tuning range exceeding 105 GHz. The variation in laser output power during the scan is also shown

This compares favourably to the widest ranges that have previously been reported for violet diode lasers [5, 24]. The diode used in the present work was reported to have a front facet reflectivity of around 50% [28] which illustrates that substantial mode-hop free tuning ranges can be obtained even without the need for costly anti-reflection coating of the diode. It is noted that the laser power falls steadily throughout the scan. This is an inherent feature of the current tuning process and restricts the scanning range in all ECDL devices which rely on this principle. Starting the scan at a higher initial injection current could result in wider tuning ranges but may limit the diode operational lifetime. Clearly, the fractional decrease in laser power is less significant the shorter the scan.

A measurement of the linewidth of the ECDL emission was made using the method described by Arnold et al. [29]. This resulted in an upper estimate of the laser linewidth of 8 MHz over a timescale of 150 ms. The technique relies on the assumption that the fundamental linewidth (typically around 100 kHz for ECDLs [23]) of the source is negligible compared to the magnitude of rapid mechanically-induced frequency jitter. The laser wavelength was tuned so that the transmitted intensity through a confocal etalon (FSR = 7.5, $F = 30$) was about 50% of the maximum, corresponding to the location of the steepest gradient on an interference fringe. As a result, any change in the laser frequency would result in a change in the intensity of transmitted light, which was monitored with a photodiode. The measured linewidth is the consequence of mechanical instabilities in the extended cavity and in the etalon used for analysis combined with fluctuations in laser intensity. Since the latter two effects are artefacts of the measurement, the actual linewidth is likely to be lower than the value reported.

Figure 4 shows a recorded LIF spectrum of the $5\,^2P_{3/2} \rightarrow 6\,^2S_{1/2}$ transition of atomic indium. The indium atoms were excited from the $5\,^2P_{3/2}$ state, which is the upper sub-level of the spin-orbit split ground state, to the $6\,^2S_{1/2}$ excited state. Through spontaneous emission, the atoms can decay back to either the $5\,^2P_{1/2}$ state by emission at 410 nm, or to the $5\,^2P_{3/2}$ state by emission at 451 nm. The photomultiplier was filtered to detect only the latter. Figure 4 shows a single scan spectrum acquired in 50 ms (offset from the baseline for clarity), a spectrum averaged over 200 individual scans, and a fit of a theoretical spectrum to the experimental data. Before averaging, the individual spectra were normalised with respect to the simultaneously acquired laser power. The spectrum is subjected to significant collision broadening at atmospheric pressure. As a result, the six hyperfine peaks appear merged into one another. The fitted spectra correspond to a non-linear

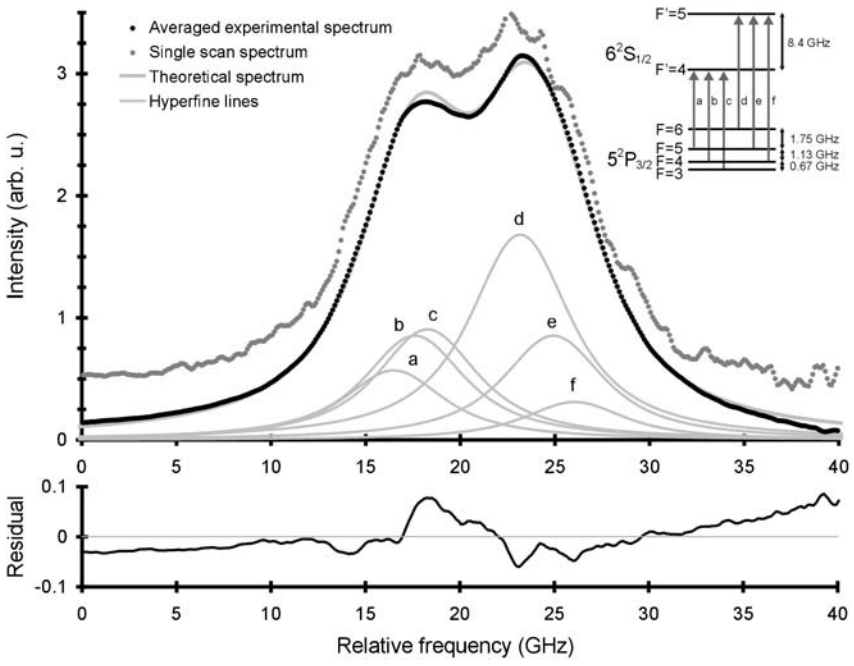

FIGURE 4 LIF spectra of the $5\,^2P_{3/2} \rightarrow 6\,^2S_{1/2}$ hyperfine structure in atomic indium, recorded in an atmospheric pressure flame at around 2000 K. Shown are a single scan spectrum and an average over 200 scans. A best fit theoretical spectrum consisting of six Voigt profiles corresponding to the six hyperfine components of the transition is also displayed. The residual of the fit is shown on a separate axis. An indium energy level diagram is shown on the *insert*

least squares fit of the sum of six Voigt profiles representing the six hyperfine transitions (see insert of Fig. 4). The relative positions of the six hyperfine peaks (hyperfine splittings of the $5\,^2P_{3/2}$ level: 1.75 GHz, 1.13 GHz, and 0.67 GHz; hyperfine splitting of the $6\,^2S_{1/2}$ level: 8.44 GHz) were taken from Deverall et al. [30] and the relative intensities (0.34; 0.51; 0.54; 1; 0.51; 0.18) of the peaks were calculated from the Clebsch-Gordan coefficients [31] of the states involved. These parameters were specified in the fit. The individual Voigt peaks are also shown and it can be seen that the composite fit is in good agreement with the experimental data (residuals less than 3%). From the shape of the hyperfine peaks, it is clear that pressure broadening is dominant under the present conditions. The Lorentzian contribution to the broadening was found to be about 5.8 GHz, whereas the Doppler broadening at 2000 K is only 2.0 GHz. Note that the higher noise level on the right-hand side of the single scan spectrum is caused by the decreasing laser power at the end of the scan resulting from tuning of the diode injection current, as discussed above.

The maximum laser irradiance used in the experiments was about 11 W cm^{-2}. The linearity of the fluorescence signal with increasing laser power was confirmed experimentally by varying the laser excitation intensity (data not shown), and no saturation was observed. Previous studies on indium LIF in similar flame environments by Dec and Keller [18] and by Engström [32] have found that no saturation is evident in the 451 nm transition of indium even for substantially greater values of laser irradiance than that used here. These findings are substantiated by theoretical calculations of the saturation irradiance, which we based on data for similar three-level systems [33, 34].

Figure 5 shows the indium LIF profile along a vertical axis near the centre of the flame, recorded by translating the burner with respect to the laser beam. Each data point shown corresponds to the integrated fluorescence signal of an averaged spectrum (200 scans), and the error bars correspond to the standard deviation of the integrated single-scan signals. The flame front is located at a height between 15 and 16 mm from the burner. Signal levels rise sharply in this high-temperature zone due to the formation of neutral indium atoms by volatilisation and decomposition of $InCl_3$ [35]. Significant fluctuation in the signal level is observed in the region immediately surrounding the flame front due to slight flickering of the flame front location, which gives rise to the larger error bars in Fig. 5 for the data points corresponding to these positions. Another reason for this fluctuation may be that the $InCl_3$ arrives at the flame front in the form of solid particulates [35], which would cause the liberation of indium atoms at the flame

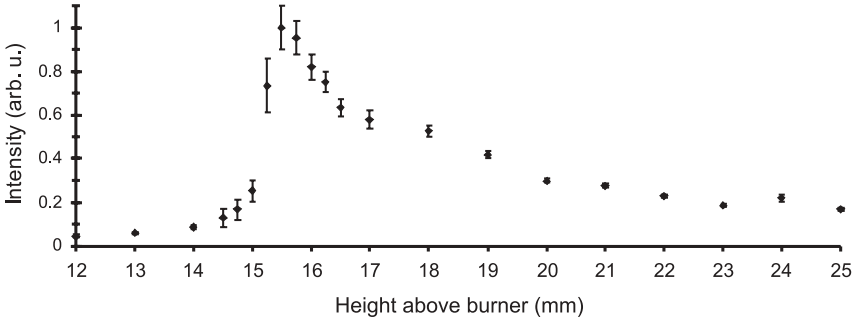

FIGURE 5 Profile of LIF signal intensity recorded along the central axis of a laminar Bunsen flame

front to occur in discrete bursts. The existence of such particles is plausible since Mie scattering of incident laser light was observed when the seeded air stream was passed through the burner without the presence of a flame (this was not observed when the nebuliser was by-passed).

The larger LIF signals observed towards the flame front are also affected by the increasing population in the $5\,^2P_{3/2}$ level state at higher temperature. This effect, however, is known to be much less pronounced than the formation of neutral indium: LIF signals observed for the $5\,^2P_{1/2} \rightarrow 6\,^2S_{1/2}$ transition, which probes the ground state, show a very similar trend to Fig. 5 [5].

The concentration of indium atoms gradually decreases with increasing height in the post flame gases. This reduction in signal strength is entirely due to indium atoms being consumed by reactions since the temperature is nearly constant in the post combustion region. The situation is likely to be similar to that in a hydrogen-air flame in which case the formation of the hydroxide InOH would be dominant [36]. The profile shown in Fig. 5 demonstrates the excellent spatial resolution (< 0.25 mm) that can be achieved using diode LIF, a significant advantage compared to the line-of-sight absorption techniques that have traditionally been employed with diode lasers in the study of flames.

4 Conclusions

Blue laser diodes are now available in the 430–450 nm spectral region and tests have been performed with a diode operating near 450 nm. A regular mode spacing of 0.058 nm was observed from the FP diode, which is multimode in free-running operation. Stable and widely tunable single-mode output and a mode-hop free tuning range exceeding 105 GHz were achieved by the construction of a Littrow configuration extended cavity around the diode. Diodes in this region hold promise for experimental applications in various situations including atomic and molecular spectroscopy and also for atom and ion cooling. The potential of this new laser has been demonstrated by performing high resolution fluorescence spectroscopy of indium atoms seeded to a flame. The 451 nm extended cavity laser is of particular interest because, used in combination with a 410 nm diode laser [5], both the $5\,^2P_{1/2} \rightarrow 6\,^2S_{1/2}$ and the $5\,^2P_{3/2} \rightarrow 6\,^2S_{1/2}$ transitions could be probed using diode based laser technology. This would allow, for example, indium atom cooling experiments to be performed using simple diode lasers, obviating the need for second harmonic generation from traditional NIR diode or Ti:Saphire laser sources [15], thus substantially reducing cost and complexity of apparatus required. Furthermore, the possibility of exciting both indium transitions with diode lasers holds promise for the development of a compact and cheap laser thermometry technique based on two-line atomic fluorescence [16]. This technique has the potential to provide accurate temperature measurements in fluctuating [16] and even sooting [17] combustion environments, with high temporal and spatial resolution. It has previously only been performed with large and expensive dye laser systems pumped by Nd:YAG or Ar^+ lasers [16, 18]. The strong LIF signals obtained from flames, which are reported here, illustrate the feasibility of such a concept.

ACKNOWLEDGEMENTS This work was sponsored by a grant from the Paul Instrument Fund of the Royal Society. ISB has been supported by an EPSRC CASE award, partially funded by Rolls-Royce. JH has been assisted by a Marie Curie Fellowship of the European Community Human Potential programme, under the contract number HPMF-CT-2002-01574. CFK gratefully acknowledges support by the EPSRC under grant numbers GR/R98679/01 and GR/R61994/01. The authors would like to thank Prof. P. Ewart for fruitful discussions and for the loan of vital experimental equipment.

REFERENCES

1 S. Nakamura: Science **281**, 956 (1998)
2 U. Gustafsson, J. Alnis, S. Svanberg: Am. J. Phys. **68**, 660 (2000)
3 H. Leinen, D. Gläßner, H. Metcalf, R. Wynands, D. Haubrich, D. Meschede: Appl. Phys. B **70**, 567 (2000)
4 O.M. Maragò, B. Fazio, P.G. Gucciardi, E. Arimondo: Appl. Phys. B **77**, 809 (2003)
5 J. Hult, I.S. Burns, C.F. Kaminski: Opt. Lett. **29**, 827 (2004)
6 H. Scheibner, St. Franke, S. Solyman, J.F. Behnke, C. Wilke, A. Dinklage: Rev. Sci. Instrum. **73**, 378 (2002)
7 J.T.C. Liu, R.K. Hanson, J.B. Jeffries: J. Quant. Spec. Rad. Trans. **72**, 655 (2002)
8 G.P.T. Lancaster, H. Häffner, M.A. Wilson, C. Becher, J. Eschner, F. Schmidt-Kaler, R. Blatt: Appl. Phys. B **76**, 805 (2003)
9 K.B. MacAdam, A. Steinbach, C. Wieman: Am. J. Phys. **60**, 1098 (1992)
10 T. Hof, D. Fick, H.J. Jänsch: Opt. Commun. **124**, 283 (1996)
11 T. Aizawa: Appl. Opt. **40**, 4894 (2001)
12 P.A. Martin: Chem. Soc. Rev. **31**, 201 (2002)
13 J.B. McManus, M.S. Zahniser, D.D. Nelson, L.R. Williams, C.E. Kolb: Spectrochim. Acta A **58**, 2465 (2002)
14 M. Tacke: Infrared Phys. Techn. **36**, 447 (1995)
15 U. Rasbach, J. Wang, R. de la Torre, V. Leung, D. Haubrich, D. Meschede, O.M. Maragò, B. Fazio, P.G. Gucciarde, F. Fuso, C. Vasi, E. Arimondo: Abstracts of the 11th MEL-ARI/NID Workshop, Toulouse, France, 5–7 February 2003
16 C.F. Kaminski, J. Engström, M. Aldén: Proc. Combust. Inst. **27**, 85 (1998)
17 J. Engström, J. Nygren, M. Aldén, C.F. Kaminski: Opt. Lett. **25**, 1469 (2000)
18 J.E. Dec, J.O. Keller: Proc. Combust. Inst. **21**, 1737 (1986)
19 See http://www.nichia.co.jp
20 S. Nagahama, T. Yanamoto, M. Sano, T. Mukai: Phys. Stat. Sol. A **190**, 235 (2002)
21 M.E. Webber, J. Wang, S.T. Sanders, D.S. Baer, R.K. Hanson: Proc. Combust. Inst. **28**, 407 (2000)
22 P. Vogel, V. Ebert: Appl. Phys. B **72**, 127 (2001)
23 C.E. Wieman, L. Hollberg: Rev. Sci. Instrum. **62**, 1 (1991)
24 L. Hildebrandt, R. Knispel, S. Stry, J.R. Sacher, F. Schael: Appl. Opt. **42**, 2110 (2003)
25 S. Nakamura, M. Senoh, S. Nagahama, N. Iwasa, T. Yamada, T. Matsushita, Y. Sugimoto, H. Kiyoku: Appl. Phys. Lett. **70**, 616 (1997)
26 U. Tisch, B. Meyler, O. Katz, E. Finkman, J. Salzman: J. Appl. Phys. **89**, 2676 (2001)
27 H.X. Jiang, J.Y. Lin: Appl. Phys. Lett. **74**, 1066 (1999)
28 Nichia Corporation: *Private communication*
29 A.S. Arnold, J.S. Wilson, M.G. Boshier: Rev. Sci. Instrum. **69**, 1236 (1998)
30 G.V. Deverall, K.W. Meissner, G.J. Zissis: Phys. Rev. **91**, 297 (1953)
31 C. Candler: *Atomic Spectra and the Vector Model* (Hilger & Watts, London 1964)
32 J. Engström: *Development of a 2D Temperature Measurement Technique for Combustion Diagnostics using 2-line Atomic Flourescence* (Thesis, Lund Institute of Technology, Lund 2001)
33 G.D. Boutilier, M.B. Blackburn, J.M. Mermet, S.J. Weeks, H. Haraguchi, J.D. Winefordner, N. Omenetto: Appl. Opt. **17**, 2291 (1978)
34 G. Zizak, J.D. Bradshaw, J.D. Winefordner: Appl. Opt. **19**, 3631 (1980)
35 C.T.J. Alkemade: *Fundamental Aspects of Decomposition, Atomization, and Excitation of the Sample in the Flame*, in: J.A. Dean, T.C. Rains (Eds.): *Flame Emission & Atomic Absorption Spectrometry*, Vol 1 (Marcel Dekker, New York 1969)
36 E.M. Bulewicz, T.M. Sugden: Trans. Faraday Soc. **54**, 830 (1958)